

## New Photorefractive Polymer Composites Doped with Liquid Nonlinear Optical Chromophores

Chil-Sung Choi\*, In Kyu Moon, and Nakjoong Kim\*

Department of Chemistry, Hanyang University, Seoul 133-791, Korea

Received March 14, 2009; Revised May 7, 2009; Accepted May 7, 2009

**Abstract:** Photorefractive polymer composites were synthesized based on poly (*N*-vinylcarbazole) (PVK) doped with liquid nonlinear optical chromophores and a sensitizer C<sub>60</sub>. PVK/liquid NLO chromophores/C<sub>60</sub> devices showed no signs of phase separation and did not require a plasticizer, such as ethylcarbazole. The composites showed 69% diffraction efficiency (C3) and a rapid response time of 46 ms (C1) in four-wave mixing experiments at a light intensity of 60 mW/cm<sup>2</sup> and a wavelength of 633 nm.

**Keywords:** photorefractive effect, liquid nonlinear optical chromophore, plasticizer, photorefractive response time, diffraction efficiency.

### Introduction

The photorefractive (PR) effect refers to spatial modulation of the refractive index in a material due to light-induced redistribution of charge.<sup>1-3</sup> Under the illumination of non-uniform light formed by the interference of two coherent laser beams, a spatially oscillating space-charge field is formed as a result of the generation and redistribution of photo-induced charges. The refractive index of the material is subsequently modulated via an electro-optic effect. Photorefractive materials exhibit several unique features including photosensitivity, reversibility, and beam amplification, and are used in optical data storage and information processing.<sup>2-7</sup>

Over the past 15 years, a considerable number of studies of photorefractive polymers have been performed, with studies of poly(*N*-vinylcarbazole) (PVK) the most common.<sup>2</sup> Nevertheless, PVK systems have several problems such as phase separation, crystallization resulting from high chromophore content, and difficulty obtaining a *T<sub>g</sub>* near room temperature when adding the plasticizer.<sup>2,8</sup> To solve these problems, we developed new liquid nonlinear optical (NLO) chromophores. Those chromophores behave as both NLO chromophores and plasticizers. A PVK/liquid NLO chromophore/C<sub>60</sub> device that we manufactured showed no signs of phase separation and did not require a plasticizer such as ethylcarbazole.

### Experimental

**Materials.** The chemical structures investigated are shown in Figure 1, although the synthesis details and photophysical properties will be published elsewhere. Chromophores were purified using column chromatography. The absorption spectra of OPEM-476 and OPEM-488 in are shown in Figure 1. The absorption spectra of OPEM-476 and OPEM-488 in solution are located at 476 and 488 nm, respectively.

Secondary standard PVK (Aldrich chem. Co. *M<sub>w</sub>*: 50,400, PDI=1.8) was purified by precipitation (precipitation three times from 15 wt% THF with MeOH).<sup>9</sup> In addition, fullerene C<sub>60</sub> was used without purification. The two chromophores were of the donor- $\pi$ -acceptor type, with 4-methylene-3-phenylisoxazolone (ISOX) and 1, 3-dimethyl-barbituric acid (DMB) acceptors, a  $\pi$ -conjugated system, and an *N, N*-bis (2-ethylhexyl) amino donor group. The 2-ethylhexyl group is a good electron donor and plasticizer, while ISOX and DMB have been used as electron accepting groups in compounds for nonlinear optics for several decades.<sup>10-12</sup>

**Sample Preparation.** The compositions of the samples were PVK/OPEM-476/C<sub>60</sub> (49.5/50/0.5 wt%)-C1, PVK/OPEM-488/C<sub>60</sub> (49.5/50/0.5 wt%)-C2, PVK/OPEM-476/C<sub>60</sub> (39.5/60/0.5 wt%)-C3, and PVK/OPEM-488/C<sub>60</sub> (39.5/60/0.5 wt%)-C4. To obtain homogeneous samples, all components were dissolved in toluene, the solvent was evaporated, and the mixture was softened at a temperature below 150 °C. The device was prepared by sandwiching the softened composite between two ITO-coated glass plates. The thickness of the film was controlled using a Teflon spacer (100  $\mu$ m) between the two ITO glass plates. The thickness of the active layer was 100  $\mu$ m. The glass transition temperature *T<sub>g</sub>* of the com-

\*Corresponding Authors. E-mails: sevenstar@hanyang.ac.kr or kimnj@hanyang.ac.kr

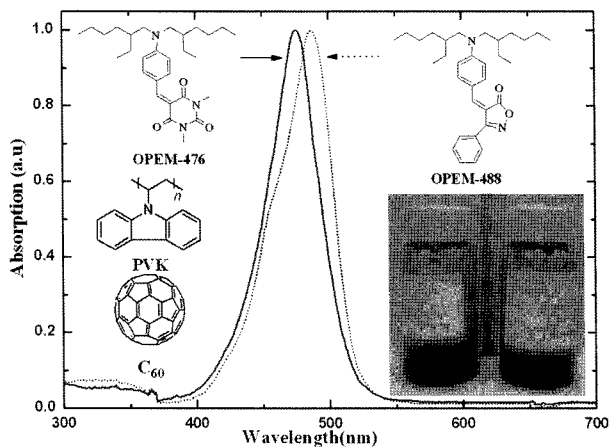


**Figure 1.** Chemical structure of the components of the PR samples [Photoconducting polymer PVK (poly(*N*-vinylcarbazole)), nonlinear optical chromophores OPEM-476 (5-(4-(bis(2-ethylhexyl)amino)benzylidene)-1,3-dimethylpyrimidine-2,4,6(1H,3H,5H)-trione) and OPEM-488 ((*Z*)-4-(4-(bis(2-ethylhexyl)amino)benzylidene)-3-phenylisoxazol-5(4H)-one), sensitizer C<sub>60</sub> (Fullerene)] and absorption spectra of OPEM-476 (solid curve) and OPEM-488 (dot curve) in methylene chloride. The inset shows phase state of chromophores (liquid phase) at room temperature.

posite determined by differential scanning calorimetry (TA Q100) was 27–29 °C (wider glass transition) at a heating rate of 10 °C/min.<sup>13–15</sup>

**Photoconductivity.** The Photoconductivity of the composites was measured at a wavelength of  $\lambda=632.8$  nm using the conventional DC technique.<sup>16,17</sup> A Beran model 205B-20R high voltage power supply, a Keithley 6485 picoammeter and LABVIEW software were used for the photoconductivity measurement. The current flowing through the sample during the illumination of light had an intensity of 39 mW/cm<sup>2</sup> at various electric fields. The photoconductivity was calculated as the difference between the presences of the light and dark current. The dark and the photoconductivity were calculated using the following equation:

$$\sigma_{ph} = Id/(VA) \quad (1)$$

where  $I$  is the current,  $d$  is the sample thickness,  $V$  is the applied voltage, and  $A$  is the laser beam area.

**Birefringence.** The electro-optical properties of the polymer sample were determined using the transmission ellipsometry technique.<sup>18</sup> The birefringence and orientational dynamics of the PR composites were measured using a high voltage power (Beran model 205B-20R or Trek model 10/10B) and a photo signal detector (Fluke 45 dual display multimeter or Tektronix oscilloscope TDS 460A). The sample was tilted to 45° and placed between the polarizer and the analyzer with the polarization set at +45° and -45°, respectively. The electric-field induced birefringence ( $\Delta n$ ) of the composite was determined from the variation of the transmitted intensity ( $T$ ) through a crossed polarizer upon the

application of an electric field, as described by the following equation:

$$T = \sin^2\left(\frac{2\pi}{\lambda} \cdot l \cdot \Delta n\right) \quad (2)$$

where  $\lambda$  is the wavelength and  $l$  is the distance of the light path.

**Four-Wave Mixing.** The diffraction efficiency of the photorefractive material was determined by the degenerate four wave mixing (DFWM) experiment.<sup>14,19</sup> A Beran model 205B-20R high voltage power and photo signal detector (Fluke 45 dual display multimeter or Tektronix oscilloscope TDS 460A) were used for DFWM measurement (LABVIEW routine.). Two coherent laser beams at the wavelength of 632.8 nm were irradiated on the sample in the tilted geometry with an incident angle of 30° and 60° with respect to the normal sample. The writing beams were both *s*-polarized and had an equal intensity of 30 mW/cm<sup>2</sup>. The recorded photorefractive grating was read out by a *p*-polarized counter-propagating beam. An attenuated reading beam with a very weak intensity of 0.06 mW/cm<sup>2</sup> was used. The internal diffraction efficiency  $\eta_{int}$  was calculated as follows:

$$\eta_{int} = I_{R, diff} / (I_{R, diff} + I_{R, trans}) \quad (3)$$

where  $I_{R, diffracted}$  and  $I_{R, transmitted}$  were the diffracted and transmitted intensities of the reading beam, respectively.

## Results and Discussion

Photoconductivity is one of the most important parameters in the photorefractive effect. The PR grating formation speed and space charge field formation are strongly dependent on photoconductive properties. The dark and photoconductivity were calculated using the eq. (1). At an intensity level of 39 mW/cm<sup>2</sup> and an applied field of 70 V/μm, the photo-

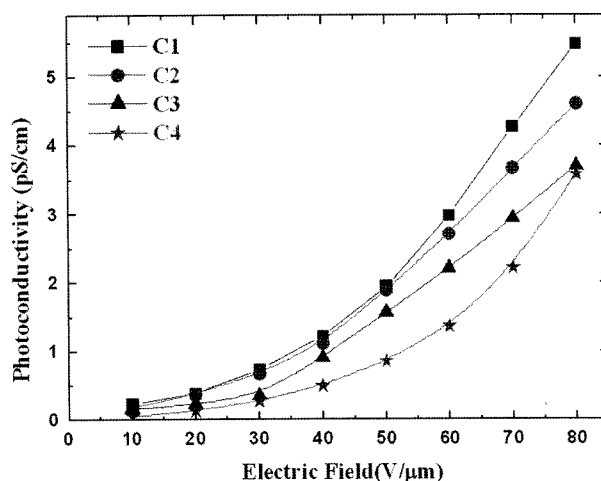


**Figure 2.** Photoconductivity as a function of electric field for composites. C1 (squares), C2 (circles), C3 (triangles), and C4 (stars). Solid lines are guides to the eyes.

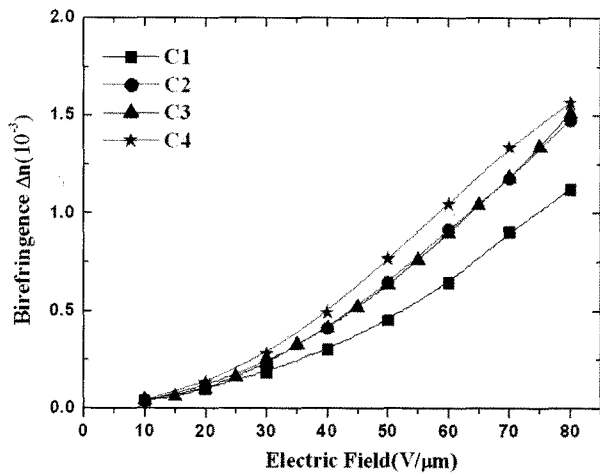


**Figure 3.** Refractive index change as a function of the electric field for composites. C1 (squares), C2 (circles), C3 (triangles), and C4 (stars). Solid lines are guides to the eyes.

conductivity of 4.27 pS/cm (C1) is two orders of magnitude larger than the dark conductivity of 0.02 pS/cm (C1) (Table I(b)). Figure 2 shows the photoconductivity as a function of an electric field for the PR composites C1-C4.

As given in Figure 3 the birefringence  $\Delta n$  of the photorefractive materials increases quadratically with an electric field in the order of  $C1 < C2 < C3 < C4$ . A figure-of-merit ( $F_{Kerr}$ ) given by eq. (2) is suitable to characterize the efficiency of the chromophores:

$$F_{Kerr} \approx \frac{2}{9MkT} [\mu_g^2 \Delta\alpha] \quad (4)$$

where  $\mu_g$  is the molecular dipole moment,  $\Delta\alpha$  is the polarizability anisotropy,  $k$  is the Boltzmann constant,  $T$  is the tem-

perature, and  $M$  is the molecular weight.<sup>2,15,20</sup> Chromophores with large  $\mu_g$  and  $\Delta\alpha$  are favorable because of the large contribution of reorientation effects to photorefractive properties. The molecular dipole moment  $\mu_g$  and the polarizability anisotropy  $\Delta\alpha$  were calculated using the semi-empirical method implemented in Materials Studio 4.1 (Vamp 10.0) with the AM1 approximation method used for geometric optimization.<sup>21,22</sup> Table I(a) show the molecular dipole moment  $\mu_g$ , the polarizability anisotropy  $\Delta\alpha$ , and the estimated figure-of-merit  $F_{Kerr}$  for the chromophores. The OPEM-488 chromophore is superior to the one with OPEM-476 regarding the figure-of-merit  $F_{Kerr}$ . Furthermore, the theoretical calculation results are consistent with the experimental results.

Photorefractive properties of various systems were characterized by the diffraction efficiency determined by the

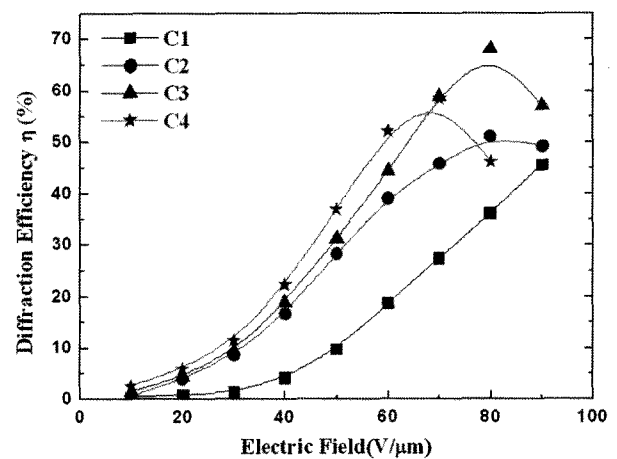


**Figure 4.** Diffraction efficiency as a function of applied electric field of the four samples C1 (squares), C2 (circles), C3 (triangles), and C4 (stars). Solid lines are guides to the eyes.

**Table I. (a) The Molecular Dipole Moment ( $\mu_g$ ) and the Polarizability Anisotropy ( $\Delta\alpha$ ) Calculated from Materials Studio 4.1 (Vamp 10.0) Using the AM1 Approximation Method for Geometric Optimization. (b) Photorefractive Properties of Composites C1-C4**

(a)							
Chromophore	$\mu_g$	$(\alpha_{xx} + \alpha_{yy})/2$	$\alpha_{zz}$	$\Delta\alpha^a$	$F_{Kerr}$		
OPEM-476	15.0	60.1	72.9	12.8	28.93		
OPEM-488	17.1	72.9	86.9	14.0	40.61		
(b)							
Composite	Concentration of Chromophores (wt %)	$\sigma_{photo}^a / \sigma_{dark}$ (pS/cm)	$\sigma_s^a$ (pS/cm/W)	$\Delta n^b$ ( $10^{-3}$ )	$\eta_{max}^c$ (%)	$\tau_1^d$ (sec)	$\tau_2^d$ (sec)
C1	OPEM-476 50 wt%	4.27/0.022	109.5	0.90	46(90 V/ $\mu$ m)	0.046	0.41
C2	OPEM-488 50 wt%	3.66/0.019	93.8	1.17	51(80 V/ $\mu$ m)	0.29	1.64
C3	OPEM-476 60 wt%	2.93/0.025	75.1	1.18	69(80 V/ $\mu$ m)	0.53	2.12
C4	OPEM-488 60 wt%	2.21/0.031	56.7	1.338	59(70 V/ $\mu$ m)	1.17	3.09

Photoconductivity  $\sigma_{photo}$ ; Dark conductivity  $\sigma_{dark}$ ; Photosensitivity  $\sigma_s$ ; Birefringence  $\Delta n$ ; Maximum diffraction efficiency  $\eta_{max}$ ; Fast response time  $\tau_1$ ; Slow response time  $\tau_2$ . SI units:  $\mu_g$   $10^{-30}$  C·m;  $(\alpha_{xx} + \alpha_{yy})/2$ ,  $\alpha_{zz}$  and  $\Delta\alpha^a$   $10^{-40}$  C·m<sup>2</sup>·V<sup>-1</sup>;  $F_{Kerr}$   $10^{-77}$  C<sup>2</sup>·m<sup>4</sup>·mol<sup>-1</sup>·kg<sup>-1</sup>;  $\Delta\alpha^a = [\alpha_{zz} - (\alpha_{xx} + \alpha_{yy})/2]$ . <sup>a</sup> $E_0=70$  V/ $\mu$ m;  $I_0=39$  mW/cm<sup>2</sup> and 25 °C. <sup>b</sup> $E_0=70$  V/ $\mu$ m;  $I_0=5$  mW/cm<sup>2</sup> and 25 °C. <sup>c</sup> $E_0=70$  V/ $\mu$ m;  $I_{write}(total)=60$  mW/cm<sup>2</sup>;  $I_{probe}(total)=0.06$  mW/cm<sup>2</sup> and 28 °C. <sup>d</sup> $E_0=70$  V/ $\mu$ m;  $I_{write}(total)=60$  mW/cm<sup>2</sup>;  $I_{probe}(total)=0.06$  mW/cm<sup>2</sup> and 36 °C.

degenerate four wave mixing (DFWM) experiment. Figure 4 shows the diffraction efficiency ( $\eta$ ) as a function of the applied electric field under stationary conditions. The maximum diffraction efficiency for four samples varied from 46-69%. The photorefractive properties of the composites are summarized in Table I(b). According to Kogelnik's coupled-wave theory,<sup>23,24</sup>  $\eta_{int}$  can be approximated by

$$\eta_{int} \propto \sin^2 \left[ \frac{\pi \cdot \Delta n(E) \cdot d}{\lambda (c_R \cdot c_S)^{1/2}} \right] \quad (5)$$

where,  $\lambda$  is the wavelength,  $\Delta n$  is the birefringence,  $d$  is the thickness of the film, and  $c_R$  and  $c_S$  are the geometrical factors. The diffraction efficiency results are consistent with the eq. (5).

The response time of the photorefractive grating recording is an important parameter in practical applications such as real-imaging and real-data processing. The curves of the PR grating formation dynamics were fitted using the following bi-exponential function:<sup>25-27</sup>

$$\eta = A \sin^2 [B \cdot (1 - m e^{-t/\tau_1} - (1 - m) e^{-t/\tau_2})] \quad (6)$$

where  $A$ ,  $B$ , and  $m$  are the fitting parameters, and  $\tau_1$  and  $\tau_2$  are the fast and slow times, respectively. Figure 5 shows a bi-exponential growth fit at an electric field of 70 V/ $\mu$ m for a total light intensity of 60 mW/cm<sup>2</sup> in sample C1 ( $\tau_1=46$  ms,  $\tau_2=491$  ms, weight factor  $m=0.39$ ). Increasing the intensity could potentially reduce the response time of our materials down to a video rate response time of 33 ms.<sup>2</sup>

Beam fanning is a noise source in photorefractive image processing and holographic storage applications. Image processing and holographic storage applications must minimize beam fanning;<sup>28,29</sup> however, it is necessary for photorefractive applications such as novelty filtering and self-phase

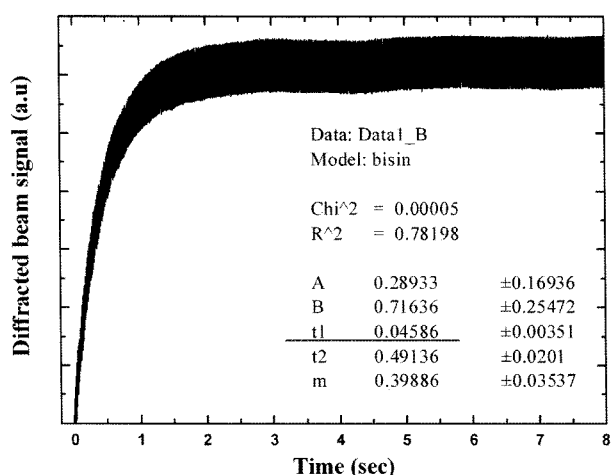


**Figure 5.** A bi-exponential growth fit (red line) to the diffraction signal (black line) at an electric field of 70 V/ $\mu$ m in a total light intensity of 60 mW/cm<sup>2</sup> in sample C1 with  $\tau_1=46$  ms,  $\tau_2=491$  ms, and weight factor  $m=0.39$ .

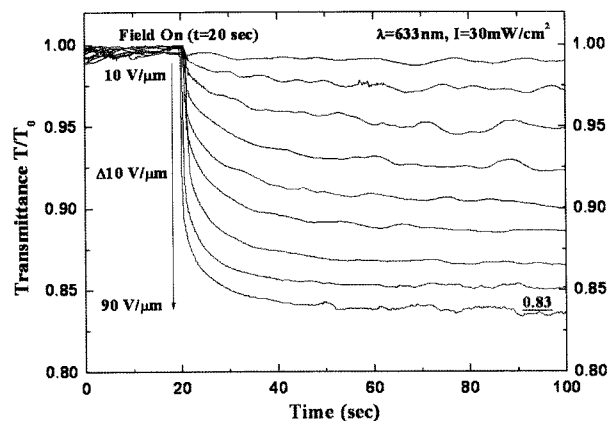


**Figure 6.** Transmitted beam power depletion in PVK/OPEM-476/C<sub>60</sub> (39.5/60/0.5 wt%) sample C3 using 633 nm s-polarized beam with intensity 30 mW/cm<sup>2</sup>.

conjugation.<sup>28-31</sup> The experimental setup used in the study is two-beam coupling (TBC) setup.<sup>30</sup> Figure 6 shows the pump beam depletion resulting from beam fanning of the PVK/OPEM-476/C<sub>60</sub> (39.5/60/0.5 wt%) sample C3 at various electric fields. At 90 V/ $\mu$ m the transmittance of the samples drops to 85% in sample C3 and 83% in sample C4. If we had adjusted the beam fanning in the sample, we would have been able to apply it to not only image processing and holographic storage applications but also novelty filtering, self-phase conjugation, and related techniques.

## Conclusions

In conclusion, we studied four PR polymer composites based on PVK which contained liquid NLO chromophores and C<sub>60</sub>. The utilization of these liquid chromophores carries the significant advantage of eliminating the need for an inert plasticizer. Glass transition temperatures  $T_g$  of the composites were lowered to near room temperature without the requirement for additional plasticizer. The PR polymer composites also possess a long shelf lifetime of over 10 months. Transient four-wave-mixing experiments found a photorefractive response dominated by a fast time constant of 46 ms at a total irradiance of 60 mW/cm<sup>2</sup>.

**Acknowledgements.** This work was supported by the National Research Foundation (NRF) grant funded by the Korea government (MEST) through the Active Polymer Center for Pattern Integration (No. R11-2007-050-01003-0). In addition, this work was supported by the Research fund of HYU (HYU-2008-T).

## References

- (1) W. E. Moerner and S. M. Silence, *Chem. Rev.*, **94**, 127 (1994).
- (2) O. Ostroverkhova and W. E. Moerner, *Chem. Rev.*, **104**, 3267

- (2004).
- (3) B. Kippelen, in *Photorefractive Materials and Their Applications*, P. Günter and J.-P. Huignard, Eds., Springer, New York, 2007, Vol. 2, pp 487-534.
  - (4) W.-J. Joo, N.-J. Kim, H. Chun, I. K. Moon, and N. Kim, *Polymer*, **43**, 9863 (2001).
  - (5) A. Goonesekera, D. Wright, and W. E. Moerner, *Appl. Phys. Lett.*, **76**, 3358 (2000).
  - (6) M. B. Klein, G. D. Bacher, A. Grunnet-Jepsen, D. Wright, and W. E. Moerner, *Opt. Commun.*, **162**, 79 (1999).
  - (7) D. H. Choi, W. G. Jun, K. Y. Oh, H. N. Yoon, and J. H. Kim, *Macromol. Res.*, **11**, 43 (2003).
  - (8) W. E. Moerner, C. Poga, Y. Jia, and R. J. Twieg, *OSA Tech. Dig. Ser.*, **21**, 331 (1995).
  - (9) D. D. Perrin and W. L. F. Armarego, *Purification of laboratory chemicals*, 3<sup>rd</sup> ed., Pergamon Press, Oxford, 1988, p 261.
  - (10) K. D. Singer, S. F. Hubbard, A. Schober, L. M. Hayden, and K. Johnson, in *Characterization techniques and tabulations for organic nonlinear optical materials*, M. G. Kuzyk and C. W. Dirk, Eds., Marcel Dekker Inc., New York, 1998, chap. 6.
  - (11) B. R. Cho, K. N. Son, S. J. Lee, T. I. Kang, M. S. Han, and S. J. Jeon, *Tetrahedron Lett.*, **39**, 3167 (1998).
  - (12) P. V. Bedworth, Y. Cai, A. Jen, and S. R. Marder, *J. Org. Chem.*, **61**, 2242 (1996).
  - (13) S. H. Lee, W. S. Jahng, K. H. Park, N. Kim, W.-J. Joo, and D. H. Choi, *Macromol. Res.*, **11**, 431 (2003).
  - (14) I. K. Moon, C.-S. Choi, and N. Kim, *J. Polym. Sci. Part A: Polym. Chem.*, **46**, 1783 (2008).
  - (15) H. Chun, I. K. Moon, D.-H. Shin, and N. Kim, *Chem. Mater.*, **13**, 2813 (2001).
  - (16) *Organic Photoreceptors for Imaging Systems*, P. M. Borsenberger and D. S. Weiss, Eds., Marcel Dekker Inc., New York, 1993, chap. 11.
  - (17) J. S. Schildkraut, *Appl. Phys. Lett.*, **58**, 340 (1991).
  - (18) A. Yariv, *Optical Electronics*, 4th ed., Harcourt Brace Jovanovich, Orlando, 1991, chap. 1.
  - (19) R. Bittner, T. K. Daubler, D. Neher, and K. Meerholz, *Adv. Mater.*, **11**, 123 (1999).
  - (20) R. Wortmann, C. Poga, R. J. Twieg, C. Geletneky, C. R. Moylan, P. M. Cotts, H. Horn, J. E. Rice, and D. M. Burland, *J. Chem. Phys.*, **105**, 10637 (1996).
  - (21) B. Martin, P. Gedeck, and T. Clark, *Int. J. Quantum. Chem.*, **77**, 473 (2000).
  - (22) T. Clark, A. Alex, B. Beck, F. Burkhardt, J. Chandrasekhar, P. Gedeck, A. Horn, M. Hutter, B. Martin, G. Rauhut, W. Sauer, T. Schindler, T. Steinke, Vamp. Version 10.0, Erlangen, 2003. This version is provided as part of Materials Studio 4.1 by Accelrys Inc.
  - (23) H. Kogelnik, *Bell Syst. Tech. J.*, **48**, 2909 (1969).
  - (24) R. Bittner, C. Brauchle, and K. Meerholz, *Appl. Opt.*, **37**, 2843 (1998).
  - (25) C. Fuentes-Hernandez, J. Thomas, R. Termine, M. Eralp, M. Yamamoto, K. Cammack, K. Matsumoto, G. Meredith, N. Peyghambarian, B. Kippelen, and S. R. Marder, *Proc. SPIE-Int. Soc. Opt. Eng.*, **5216**, 83 (2003).
  - (26) C.-S. Choi, I. K. Moon, and N. Kim, *Appl. Phys. Lett.*, **94**, 053302 (2009).
  - (27) J.-W. Oh, J.-W. Choi, and N. Kim, *Macromol. Res.*, **17**, 69 (2009).
  - (28) Megan, R. Leahy, and David J. McGee, *Opt. Commun.*, **187**, 277 (2001).
  - (29) A. Grunnet-Jepsen, C. L. Thompson, R. J. Twieg, and W. E. Moerner, *J. Opt. Soc. Am. B*, **15**, 901 (1998).
  - (30) G. J. Salamo, M. J. Miller, W. W. Clark III, G. L. Wood, and E. J. Sharp, *Opt. Commun.*, **59**, 417 (1986).
  - (31) M. J. Miller, G. L. Wood, and G. J. Salamo, *Mat. Res. Soc. Symp. Proc.*, **479**, 193 (1997).